CHARGE DIVISION USING CARBON FILAMENTS FOR OBTAINING COORDINATE INFORMATION FROM DETECTION OF SINGLE ELECTRONS*

F. BIRD, S. SHAPIRO, V. ASHFORD, D. McSHURLEY, R. REIF, D.W.G.S. LEITH, S. WILLIAMS

Stanford Linear Accelerator Center, Stanford University, Stanford, California 94305

ABSTRACT

Seven micron diameter Carbon filaments forming the anode of a multiwire proportional chamber have been used to detect single electrons. Charge division techniques applied to the 5 cm long wire resulted in a position resolution of $\sigma/L < 2\%$ for a collected signal charge of 30 fC.

1. Introduction

Concurrent with the development of high energy accelerators such as the Stanford Linear Collider (SLC), basic research work is progressing on the experimental detectors which will extract the physics from the particle interactions. The SLD detector at Stanford is being constructed to permit precise, exhaustive studies of the decays of the neutral weak vector boson, the Z^0, and as part of its design, a Cerenkov Ring Imaging Detector (CRID) is being constructed. The CRID, in coordination with the SLD vertex detector, will provide excellent particle identification over a wide momentum range.

Cerenkov Ring Imaging counters, as originally proposed by J. Séguinot and T. Ypsilantis,[1] are designed to measure the Cerenkov angles of photons from relativistic charged particles. By focussing the Cerenkov light from particles which traverse a radiating medium, a ring of photoelectrons can be generated in a detector which is photosensitive in the emission spectral region. In the CRID case, use of an organic chemical (TMAE) which photoionizes in the far ultraviolet, *i.e.*, wavelengths < 2200 Å, allows a very efficient, as high as 50%, photogeneration of single electrons. These photoelectrons are captured in a gas-filled time projection chamber (TPC), drifted to a multiwire proportional chamber, and amplified in the gas for readout (Fig. 1).

The initial photoconversion point of the electrons must be reconstructed with good accuracy. (Errors must be kept to $\sigma_z \approx \sigma_y \approx \sigma_z \approx 1$ mm). Two spatial coordinates are measured, one from the drift time of the electron to the PWC (relative to a trigger), and the other from the sensing wire position. To avoid parallax errors in ring reconstruction, third coordinate information is essential. The third coordinate, the conversion point of the electron in the depth of the TPC, requires a knowledge of the avalanche position along the sense wire. In the CRID, designed to operate where TMAE has an ≈ 2 cm absorption length dictating a TPC depth of 5 to 8 cm, the sense wires are very short.

To make the depth measurement, *i.e.*, to measure the position of an avalanche along a sense wire, two methods have been used successfully in practice. Cathode pad readout, where the motion of the positive ion cloud as it moves away from the sense wire induces a positive charge on a conducting electrode, has been extensively used and is well understood. Also well understood, is the charge division technique, where the sense wire is resistive and the avalanche current is divided between ends of the sense wire depending on the avalanche location. For short sense wires, as in the CRID case, conventional resistive stainless steel (or tungsten) wires would have very low resistance, causing the S/N ratio to be too small to obtain the required precision in the charge division measurement. A method of charge division using a carbon fiber as the sense wire has been developed at SLAC and will be reported here.

This paper will first review the charge division technique and the relevant noise issues. Then the equipment and experimental technique will be described and results of charge division performance tests on both the bench, and in a CRID chamber, presented. A short summary with a discussion of future development work to be undertaken will conclude.

2. Charge Division

The charge division technique relates the difference between charges detected at the two ends of a sense wire to the position of the avalanche along the wire. The charge asymmetry A_Q is given by

$$A_Q = \frac{Q_R - Q_L}{Q_R + Q_L} \tag{1}$$

where Q_R, Q_L are the right and left charges, respectively. The charge is measured by integrating the current signal from two very low noise amplifiers at each end of the sense wire, as shown schematically in Fig. 2. If the resistance of the wire is large
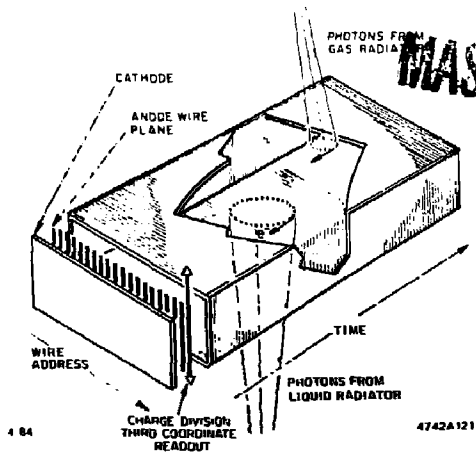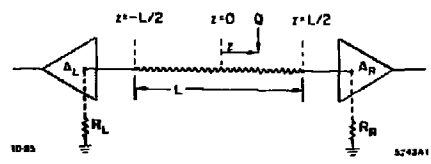

Fig. 1. CRID TPC and detector.

Fig. 2. Charge division measurement.

compared with the amplifier input impedance, then the position of the avalanche is just

$$z = \frac{L}{2} A_Q \qquad (2)$$

where z is the distance along the wire of length L, with respect to the center of the wire. The amplifier input impedance introduces a nonlinearity near the end of the sense wire. For the carbon fibers used here, this effect is negligible since the fiber resistance is about 100 times the input impedance of the amplifier. This implies that the range of A_Q is from -1 to 1.

The error in position is, from (1) and (2),

$$\frac{\sigma_z}{L} = \frac{\sigma_A}{2} = \frac{\sigma_Q}{Q} \qquad (3)$$

where $Q = Q_R + Q_L$ is the total charge, and σ_Q, the error in the charge measurement, is

$$\sigma_Q = \sqrt{\sigma_J^2 + (\frac{Q_L}{Q_R + Q_L})^2 \sigma_R^2 + (\frac{Q_R}{Q_R + Q_L})^2 \sigma_L^2} \qquad (4)$$

for σ_J the Johnson noise contribution, which is independent of the avalanche position along the sense wire, and $\sigma_{R,L}$ the amplifier input noise contribution of the right(left) channel (right and left are arbitrary).

Then, by measuring A_Q as a function of wire position, all the performance parameters for the carbon wire charge division can be determined.

3. Noise

Noise in the charge measurement limits the resolution. There are two forms of noise in the charge division technique. The thermal, or Johnson, noise of the sense wire is a source of parallel noise. The electronic noise from the amplifier is a series noise source.

The equivalent noise charge (ENC) for the RC-CR shaping electronics used here (see section 5) is given by:[2]

$$ENC = 2.7 \times \sqrt{\frac{kT\tau}{2R_w} + \frac{kTR_sC_{in}^2}{2\tau}} \qquad (5)$$

where R_w is the sense wire resistance in this charge division technique (the other end of the wire is a virtual ground), R_s is the input FET channel noise resistance, C_{in} is the input capacitance, including that of the FET, seen by the input stage, τ is the shaping time constant of the circuit, k is Boltzmann's constant, and T is the temperature.

The CRID chamber gain must be kept to a few $\times$ 10⁵, as higher gains give rise to a large number of avalanche induced ultraviolet photons, converting in the TMAE creating non-Cerenkov photoelectrons; a severe source of background. RMS noise levels then, must be a few $\times$ 10³ electrons in order to achieve resolutions on the order of one percent. The wire resistance necessary to give a 1% measurement of avalanche for a signal of 2×10^5 electrons can be estimated position using (5). The rms noise must not exceed 2000 electrons, by (3), for the worst case of a signal at one end of the wire. [The FET noise, for $\tau \approx 50$ nsec, is estimated to be $\approx$1000 electrons; then by (5), $R_w \approx 15$kΩ.]

4. Carbon Fibers

For a short sense wire, a high resistivity material must be used for the wire, to keep the Johnson noise level small. Elemental carbon has the appropriate bulk resistivity. For example, a 5 cm long 20μm wire would require a material of 9200 μΩ-cm resistivity, a value typical of a semiconductor, to get 15kΩ. Carbon has a resistivity of about 1600 μΩ-cm, implying that a 7μm diameter fiber will have a resistance in the right range, specifically R_w=20.9kΩ. A comparable 20μm stainless steel wire would have about 75Ω resistance, which is far too small.

A sample of 7μm diameter wire was obtained from American Cyanamid Corporation. The wire is a nickel-coated carbon fiber which is marketed as a lightweight, rugged conductor for use as an EMI shield for personal computers, etc. The specifications are listed in Table I. The maximum breaking tension is about 13 grams, corresponding to a breaking strength of 450,000 psi. The fibers are delivered in a bundle, and the filaments used were selected at random.

TABLE I

Carbon Filament Properties	
Source	American Cyanamid
Diameter	7 μm
Breaking Strength	450,000 psi
Elongation	1.5%
Carbon Resistivity	1600 μΩ-cm
Coated Resistivity	26 μΩ-cm

The nickel coating is very important. It allows solder connection with conventional lead-tin solders to the filaments. The nickel is easily removed by exposure to nitric acid from the tip of a hypodermic needle. The fibers do not deform or break during the nickel etch, and are very resilient to small transverse displacements delivered by the tip of a hypodermic needle, when viewed with a low power microscope.

5. Experimental Apparatus and Calibration

A single wire chamber was built to approximate the one which may be used in the actual SLD CRID device (Fig. 3). An aluminum cathode, 5 cm in length with a 2 mm wire-to-cathode spacing, was fit into a G-10 carrier equipped with Lemo connectors, and enclosed in a Faraday cage. Cables routed the signal to the amplifiers mounted in a nearby NIM crate. The amplifiers were not mounted right at the sense wire for mechanical reasons, not an optimal design. The chamber gas was a 70/30 mixture of methane/isobutane. The 4.5 cm of carbon used in the test cell was well within the 90 cm critical length limit[3] calculated at the breaking tension of 13 gm, so that the fiber would not be subject to electrostatic instability. The carbon fiber was strung to 11 grams of tension and its resistance was measured to be R_w=19kΩs.
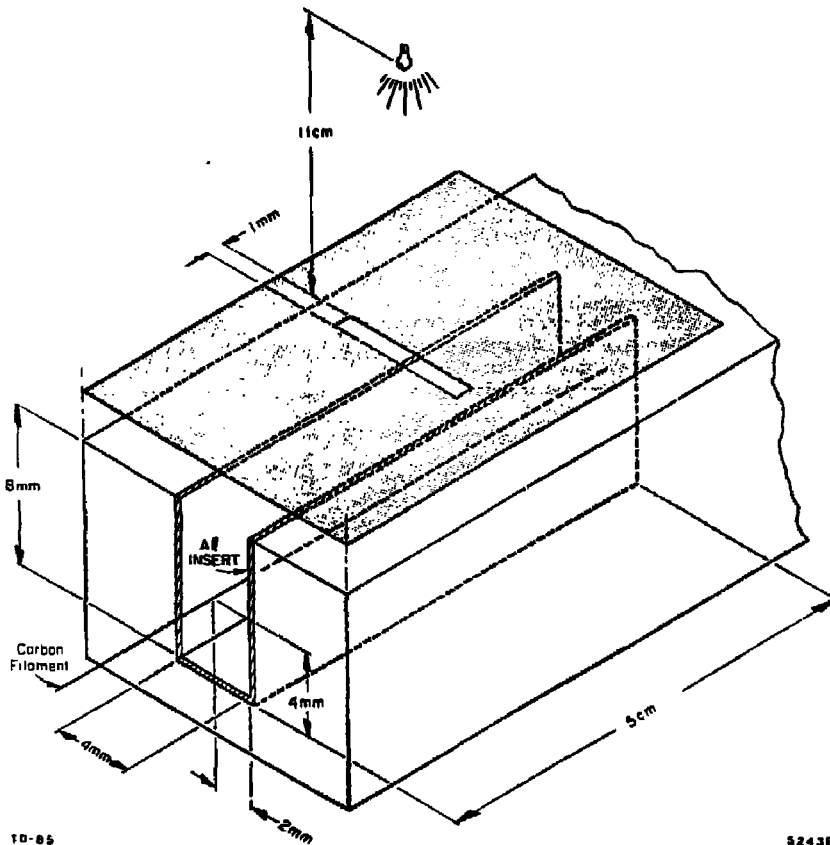
Fig. 3. Bench test carbon filament chamber.

The single photoelectrons were produced by illuminating the cathode with an ultraviolet lamp through a slit and an Aclar window. The light source was a commercial DC EPROM erasing lamp. A problem with this method was that the aluminum was reflective and produced some background to the signal, to be discussed later.

The low noise amplifier used was the HQV810 from LeCroy Research.[4] The schematic of the circuit is shown in Fig. 4. The signal was shaped to have a 26 nsec rise time and a 60 nsec decay time. From the LeCroy specification sheet, and using $\tau = 45$ nsec., the mean time of the shaping filters, the channel resistance of the input FET is calculated to be $R_s \approx 40\Omega$s. The capacitance of the input cables was measured to be 23 pF. Assuming 20 pF of on chip capacitance, Eq. (3) gives ENC = 1588 electrons per channel.
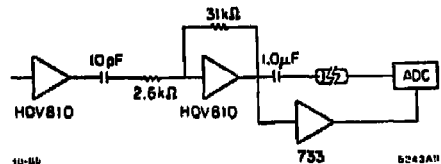

Fig. 4. Bench test electronics.

The output of each channel was input to an ADC and to a low gain amplifier stage (a 733 stage with a gain of 7). The outputs of the two low gain stages were summed and became a total pulse height trigger for the data acquisition system. The bench data were taken with a LeCroy 2249A ADC, and sent to an Apple II/Plus computer through a CAMAPPLE interface[5]. The data analysis and graphics were done with the Apple.

- 3 -

The gain of the electronics was measured by attenuating NIM level pulses and presenting that voltage to a 5 pf capacitor, connected to the amplifier input. As the amount of attenuation was changed, the input charge varied and calibration curves were generated for both signal channels independently. The calibration points were fit with a quadratic for low ADC counts and then mapped onto a linear curve for larger pulse heights (> 85 counts). The charge gain of the circuit was 2500 fC/fC. Then the two channels were given known charges simultaneously, so that charge division could be simulated. From the width of the measured A_Q distribution, which should be $\simeq 0$, the noise per channel was extracted, and found to be about 1600 electrons per channel, consistent with the expectations based on the LeCroy specifications.

6. Charge Division Performance

With the light source positioned above the slit and over the wire, single photoelectron pulse height spectra were measured at several chamber voltages. The spectra obtained were well fit by a gamma distribution,

$$P(n) = \frac{b^b}{\bar{n}\Gamma(b)}(\frac{n}{\bar{n}})^{b-1}e^{\frac{-nb}{\bar{n}}} \qquad (6)$$

where n is the pulse height, $\bar{n}$ is the mean of the pulse height, and b is a parameter which was typically about 2.5. This behavior was consistent as long as the chamber gain was high enough to generate a peaked distribution. For low voltages and no observed peaking, a simple exponential pulse height distribution was observed. The mean values of these distributions were defined to be the charge gains of the chamber. Since the gamma distribution is continuous down to zero pulse height, there were always a number of pulse heights which were too small to measure because of electronic thresholds. A peaked distribution indicated that a majority of the pulse heights were being measured, i.e., a peaked distribution implied a "plateaued" chamber. The higher the peak, the more pulses measured, but once peaked, the number of additional electrons detected as the peak of the spectrum increased was at the few percent level. A pulse height distribution and a pulse height mean versus chamber voltage plot are shown in Fig. 5. Since the Johnson noise is constant, independent of pulse height, the S/N ratio is expected to get worse as the voltage on the chamber is lowered. Furthermore, at a fixed voltage the charge division precision should vary. Figure 6 shows a scatterplot of pulse height versus A_Q. The distribution is broad for small pulse heights and very narrow for large pulses. For the largest pulses, the signals are saturated and the no measurement is possible. The points in the scatterplot away from the central distribution were attributed to photons which were reflected from the cathode and converted at some other point in the cell, away from the collimation slit. There may also have been some multiple electron avalanches at different locations on the wire. However, the ratio of the number of noise hits to signal hits did not vary as a function of pulse height, even though statistics were low, so that the noise hits are just an artifact of the technique.

For each measurement then, a mean standard deviation, (σ_A) is computed. This number is just the weighted quadrature
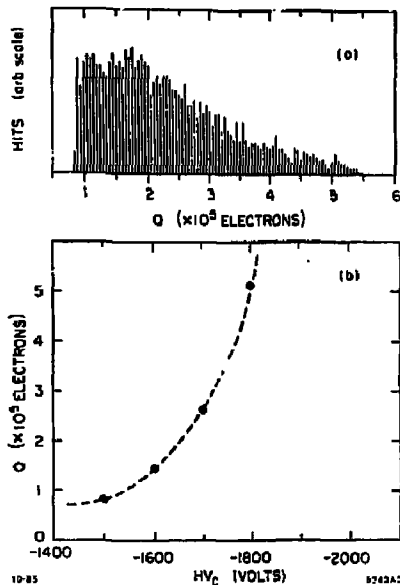

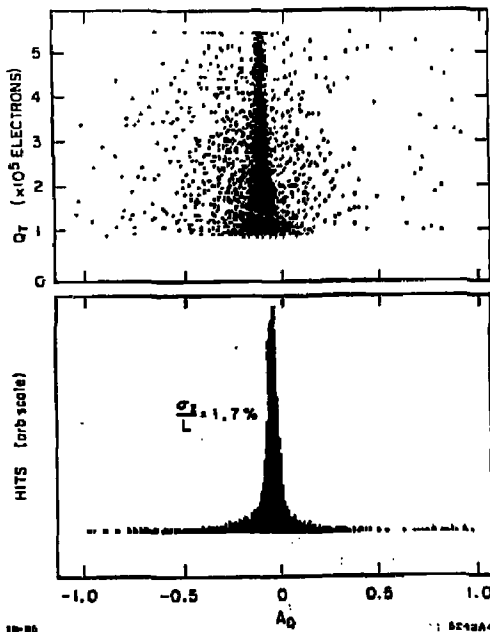Fig. 5. (a) Typical pulse height spectrum, and (b) gain versus chamber high voltage.

Fig. 6. (a) Pulse height versus A_Q, and (b) A_Q at wire center.

-4-

sum of the widths of five pulse height regions of the scatterplot, from threshold to just before saturation. At a mean gain of 2×10^5 the mean error was calculated to be 1.7% in the wire length, the contribution to the error growing quickly as the pulse height decreased, as expected. Figure 7 shows the distribution
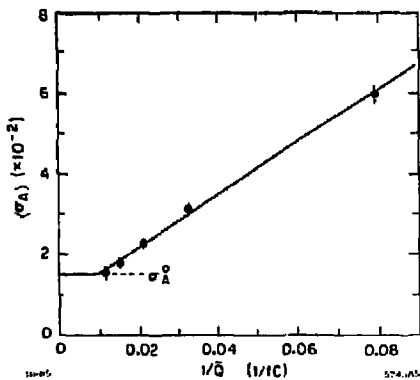

Fig. 7. $\langle \sigma_A \rangle$ versus chamber gain.

of $\langle \sigma_A \rangle$ as a function of chamber gain. The behavior is as expected, i.e., $\sigma_A \propto \frac{e_Q}{Q}$. A complete understanding of the plot requires a knowledge of the contributing error sources. There are three sources:

1. The Johnson noise of the resistive carbon filament.

2. The electronic noise from the amplifiers.

3. The distribution of avalanches due to imperfect source collimation. This spread arises from the fact that a 1 mm slit introduces a constant σ_z and hence a constant σ_A. This is indicated by σ_A^0 in the figure.

The contributions of the independent error sources, their quadrature sum, and the data are shown as a function of pulse height in Fig. 8. The errors have been converted into equivalent position errors along the wire. The plot is for the case of illumination of the central section of the wire, and the total expected noise, as computed from equations (3),(4), and (5). The measurement agrees well with the expectation. The errors in this plot are primarily due to uncertainties in the value of the total charge (especially at low total charges), and to uncertainties in the extrapolated value of R_s and in the "averaged" τ value of the shaping used.

Figure 9 is a graphic display of the performance. Figure 9(a) displays the peaks in the A_Q distributions as the source is scanned along the wire. Figure 9(b) is a plot of the linearity of the measurement for a more complete set of source positions.

7. Multiwire Chamber Measurements

Subsequent to the completion of the single filament bench tests, a prototype of the SLD CRID TPC was instrumented with a charge division detector. A multi-wire proportional chamber was built and strung with 7μm carbon filaments at a 3.2 mm pitch (see Fig. 1). (See the talk of V. Ashford, et al., in these proceedings for a complete description of the CRID device.)
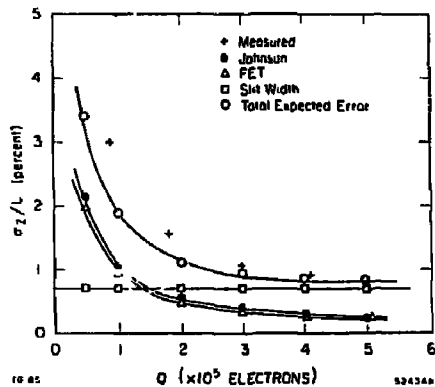

Fig. 8. Noise versus chamber gain.
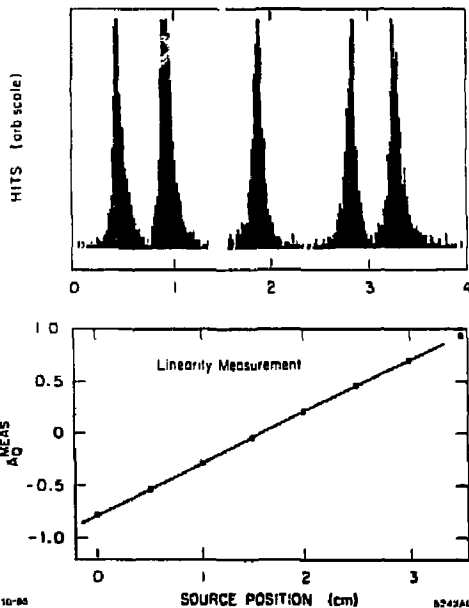

Fig. 9. (a) A_Q versus source position, and (b) linearity of A_Q.

The chamber cathode was nickel-plated aluminum. A total of 64 wires were strung to a tension of 6.5 grams each and instrumented with the HQV810 electronics. (Figure 10). Sixteen of the wires were connected to LeCroy 2241 Image Chamber Analyzers, (ICAs), which are fast (50 MHz) CAMAC controlled waveform samplers, and enable a pulse height measurement from each end of the sense wire. The charge division parameters and the avalanche position along the wire are determined in software. The gas filling used in this beam test was a 90/10 mixture of methane/isobutane with a small percentage of TMAE to detect Cerenkov photons from two radiating sources, a liquid radiator of flourocarbon, C_6F_{14}, and a gaseous radiator of isobutane.
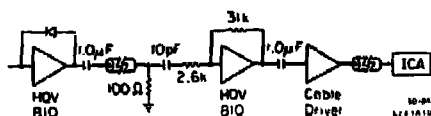
Fig. 10. CRID test electronics.

The Cerenkov light from the liquid forms a proximity focussed image on the drift box. The liquid radiator photons are incident at a steep angle to the drift box. The long mean free path for photoconversion in the TMAE gas gives rise to a large parallax error in the Cerenkov angle measurement which the third coordinate information will correct. Figure 11 displays the improvement in the width of the measured Cerenkov angle when the carbon fiber detector information is used. The width of the Cerenkov angle without the third coordinate information was measured to be $\sigma_\theta \approx 2.2°$. With the third coordinate data, a value of $\sigma_\theta \approx 0.73°$ was expected and the measurement gave $\sigma_\theta \approx 0.83°$. The result is still preliminary and analysis of the data is continuing to see if further improvements can be made.
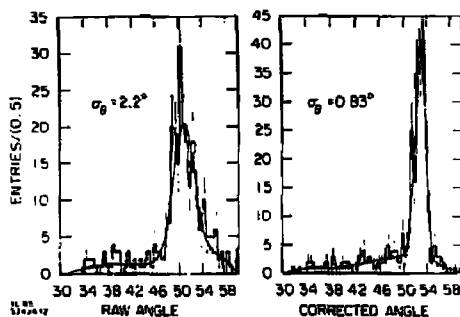

Fig. 11. Liquid ring Čerenkov angle with and without third coordinate measurement.

8. Conclusions

A new technique for determining the position of an avalanche along a sense wire in a proportional chamber has been developed. The method uses carbon filaments as sense wires and allows better than a 2% measurement of the avalanche position along the short filament from a single electron in a wire chamber operating at a gas gain of about 2×10^5. The filaments are strong and reliable. However, thicker filaments would be even stronger and tests are planned to investigate the performance of larger radius fibers, subject to their availability. Questions of lifetime and performance degradation over time remain unresolved, but will be addressed in the near future. Nonetheless, the present studies indicate that the use of carbon filaments in ring imaging Cerenkov detectors promises to be a robust, accurate, and inexpensive solution to the third coordinate problem.

References

1. J. Séguinot and T. Ypsilantis, *Nucl. Instru. Methods* 142 p. 370, 1977.

2. C. F. G. Delaney, *Electronics for the Physicist*, Chichester, England: Ellis Horwood Limited, 1980, p. 261.

3. F. Sauli, "Principles of Operation of Multiwire Proportional and Drift Chambers," CERN 77–09, p. 57, May 1977.

4. LeCroy Research Systems Corp. Technical Data Sheet, "The Model HQV810 8 Channel Hybrid Preamplifier," copyright March 1984.

5. S. H. Williams, *et al.*, "CAMAPPLE: CAMAC Interface to the Apple Computer," SLAC-PUB-2728, pp. 1-5, September 1981.